

Applying Grover-mixer Quantum Alternating Operator Ansatz Algorithm to High-order Unconstrained Binary Optimization Problems

Evgeniy O. Kiktenko,* Elizaveta V. Krendeleva, and Aleksey K. Fedorov
National University of Science and Technology “MISIS”, Moscow 119049, Russia

The Quantum Approximate Optimization Algorithm (QAOA) is among leading candidates for achieving quantum advantage on near-term processors. While typically implemented with a transverse-field mixer (XM-QAOA), the Grover-mixer variant (GM-QAOA) offers a compelling alternative due to its global search capabilities. This work investigates the application of GM-QAOA to Higher-Order Unconstrained Binary Optimization (HUBO) problems, also known as Polynomial Unconstrained Binary Optimization (PUBO), which constitute a generalized class of combinatorial optimization tasks characterized by intrinsically multi-variable interactions. We present a comprehensive numerical study demonstrating that GM-QAOA, unlike XM-QAOA, exhibits monotonic performance improvement with circuit depth and achieves superior results for HUBO problems. An important component of our approach is an analytical framework for modeling GM-QAOA dynamics, which enables a classical approximation of the optimal parameters and helps reduce the optimization overhead. Our resource-efficient parameterized GM-QAOA nearly matches the performance of the fully optimized algorithm while being far less demanding, establishing it as a highly effective approach for complex optimization tasks. These findings highlight GM-QAOA’s potential and provide a practical pathway for its implementation on current quantum hardware.

I. INTRODUCTION

Quantum computing has emerged as a transformative paradigm for addressing computational challenges that are intractable for classical systems. In the noisy intermediate-scale quantum (NISQ) era, variational quantum algorithms (VQAs) have become a cornerstone for practical applications [1, 2], demonstrating promise in areas such as quantum machine learning [3], quantum chemistry [4], quantum simulation [5], and linear algebra [6]. By harnessing the principles of quantum mechanics, such as superposition and entanglement, quantum processors promise to deliver substantial speedups in these and other domains, including cryptography, material science, and optimization [7].

Among the most promising approaches for near-term quantum devices is the Quantum Approximate Optimization Algorithm (QAOA) [8], which has been theoretically shown to hold potential for quantum advantage [9] and has been successfully implemented on various quantum hardware platforms [10–12]. In the literature, the acronym “QAOA” appears in two closely related forms: *Quantum Approximate Optimization Algorithm*, emphasizing its goal-oriented nature, and *Quantum Alternating Operator Ansatz*, highlighting the alternating structure of cost and mixer unitaries. The latter viewpoint has become increasingly relevant as generalized, problem-aware mixers have been developed to extend QAOA beyond the standard transverse-field construction.

A prominent example of such generalization is the Grover-Mixer QAOA (GM-QAOA), which replaces the transverse-field mixer with a Grover-style diffusion operator [13–20] (see also Fig. 1). The conceptual foundation for using Grover-based amplitude amplification in quantum simulation and optimization was previously demonstrated in the context of finding low-energy states of disordered Ising models [21], highlighting its potential beyond unstructured search. Unlike the standard mixer, which acts locally and updates qubits independently, the Grover mixer performs a global transformation that collectively rotates amplitudes across the entire computational basis. This global mixing dynamically couples all basis states, enabling more effective exploration of complex energy landscapes and potentially accelerating convergence. A growing body of work has examined the properties and limitations of Grover-type mixers. Analytical studies indicate that GM-QAOA performance is largely influenced by the statistical structure of the cost landscape, and that Grover mixers can offer at most quadratic sampling advantages, while typically requiring exponentially increasing depth to maintain a fixed approximation performance [15, 16]. Extensions such as threshold-based mixers have been proposed to improve parameter selection and empirical behavior in specific regimes [17], while numerical investigations have highlighted distinctive features including significantly fairer sampling across degenerate optima compared to transverse-field QAOA (XM-QAOA) [19]. More recent analytical treatments have clarified the inherently non-local structure of multi-layer Grover mixers and their connections to higher-order interactions in the underlying

* Correspondence email address: evgeniy.kiktenko@gmail.com

hypergraph [20]. In parallel, Lie-algebraic analysis has demonstrated that GM-QAOA possesses unusually rich dynamical expressivity: its dynamical Lie algebra is maximal among QAOA variants initialized with the same state, yielding explicit characterizations of conserved quantities and even provable avoidance of barren plateaus for broad classes of objective functions [22]. Taken together, these results provide a comprehensive and nuanced picture of both the strengths and the intrinsic limitations of Grover-type mixers in variational quantum optimization.

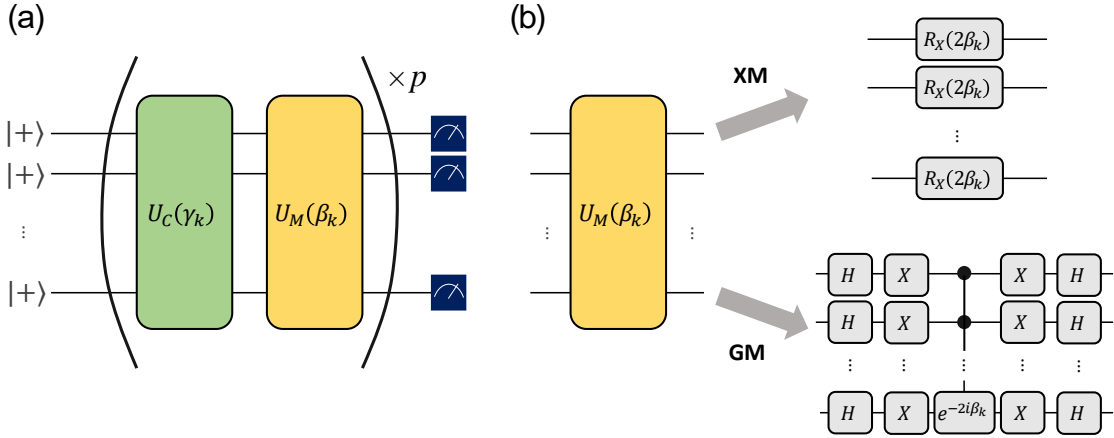


Figure 1: (a) General structure of the QAOA circuit. (b) Two implementations of the mixing operator considered in this work: the standard transverse-field mixer (leading to XM-QAOA) and the Grover-type mixer (leading to GM-QAOA). Standard notation is used for the Hadamard gate, rotations about the Bloch x axis, the Pauli- X (inversion) gate, and the multi-controlled phase gate.

A commonly noted limitation of the Grover mixer is its intrinsic non-locality: implementing the corresponding diffusion operator generally requires highly entangling multi-qubit operations, in stark contrast to the transverse-field mixer composed of simple single-qubit rotations. Such non-local structure makes the Grover mixer reminiscent of complex multi-controlled gates, including generalizations of the Toffoli gate. Nevertheless, recent theoretical [23–26] and experimental [27, 28] progress in qudit-based architectures demonstrates that multi-qubit entangling operations can be substantially simplified when higher-dimensional degrees of freedom are available. These developments suggest that the hardware cost of implementing Grover-type mixers may be mitigated in emerging multi-level quantum platforms.

This naturally raises the question of which classes of optimization problems can benefit most from globally acting mixing operations. A particularly promising direction is provided by problems whose objective functions contain inherently non-local interactions. Higher-Order Unconstrained Binary Optimization (HUBO) problems, also referred to as Polynomial Unconstrained Binary Optimization (PUBO), constitute a broad and practically relevant class in this category, as they explicitly incorporate interactions among more than two binary variables. Such higher-order structure goes beyond the pairwise couplings typical of QUBO formulations and naturally aligns with mixing strategies capable of exploring the configuration space in a more collective manner. These problems have attracted attention not only in quantum computing but also in alternative hardware paradigms, such as optical-inspired analog simulators [29]. While any HUBO can, in principle, be mapped to an equivalent Quadratic Unconstrained Binary Optimization (QUBO) problem through the introduction of auxiliary variables – a foundational technique established in classical optimization theory [30–32] and refined for modern hardware [33] – this mapping comes with significant overhead. It increases the problem dimension and can introduce a more complex, albeit quadratic, energy landscape. Therefore, working directly with the native HUBO formulation is theoretically appealing for quantum algorithms capable of handling high-order interactions, as it avoids this overhead and preserves the original problem’s structure. Such higher-order terms arise naturally in diverse application domains, including machine learning (e.g., higher-order feature interactions and tensor factorization) [34–36], computational biology (e.g., multi-residue energy models) [37, 38], and logistics and scheduling problems with complex multiway constraints [39, 40]. A canonical and notoriously hard combinatorial benchmark is the Low-Autocorrelation Binary Sequence (LABS) problem, which is naturally expressed as a quartic (4th-order) binary optimization problem and has recently been addressed using quantum algorithms [41]. Compared to their quadratic counterparts (QUBO), HUBO formulations can more faithfully

encode realistic dependencies, but at the expense of substantially increased combinatorial complexity: both the number of interaction terms and the ruggedness of the energy landscape typically grow rapidly with interaction order. Consequently, designing efficient quantum optimization strategies for HUBO models is of both practical relevance and fundamental theoretical interest, and provides a natural setting in which to evaluate the capabilities of global mixing mechanisms such as the Grover mixer.

In this work, we perform a detailed investigation of Grover-mixer QAOA applied to representative HUBO problem classes. Our comprehensive numerical study shows that GM-QAOA, unlike standard XM-QAOA, exhibits a monotonic improvement in performance with circuit depth and achieves superior results for models with high-order interactions. An additional contribution of this work is the development of an analytical framework for modeling the dynamics of GM-QAOA layers, which enables accurate classical approximation of near-optimal parameters and thereby reduces the overhead associated with variational optimization. We demonstrate that this resource-efficient parameterization scheme achieves performance close to that of fully optimized GM-QAOA while requiring significantly fewer circuit evaluations, making it far less demanding in experimental settings. Together, these results highlight the potential of Grover-type global mixers for tackling complex high-order optimization landscapes and provide a practical pathway for implementing GM-QAOA on near-term quantum hardware.

This paper is organized as follows. In Section II, we provide the necessary preliminaries on HUBO problems and the GM-QAOA framework. Section III presents a comparative analysis of GM-QAOA and standard XM-QAOA on a set of HUBO instances. Section IV is dedicated to our analytical contribution: we develop a mathematical model of the GM-QAOA dynamics and present a resource-efficient strategy for approximating optimal algorithm parameters. In Section V, we analyze the performance of GM-QAOA using analytically pre-optimized parameters, and benchmark this approach against constant-parameter and fully optimized QAOA variants across different problem sizes and Hamiltonian localities. Finally, we conclude in Section VI with a summary of our findings and an outlook on future research directions.

II. PRELIMINARIES

A. HUBO problems

HUBO represents a significant generalization of the well-studied QUBO framework. While QUBO problems are restricted to pairwise interactions between binary variables, HUBO problems capture complex multi-variable correlations through higher-degree polynomial terms. This extension enables more accurate modeling of real-world optimization challenges where simultaneous interactions among multiple entities play a crucial role.

Formally, a HUBO (PUBO) problem is defined as the minimization of a real-valued pseudo-Boolean function. The cost function $E : \{\pm 1\}^n \rightarrow \mathbb{R}$ can be written in the spin representation as

$$E(\mathbf{s}) = \sum_{d=1}^D \sum_{i_1 < \dots < i_d} J_{i_1 \dots i_d} s_{i_1} \dots s_{i_d}, \quad (1)$$

where $\mathbf{s} = (s_1, \dots, s_n)$ is a configuration of spin variables $s_i \in \{\pm 1\}$, $J_{i_1 \dots i_d}$ are real interaction coefficients, and D is a HUBO order parameter. Throughout this work, we denote the objective by $E(\mathbf{s})$ to emphasize its interpretation as an energy function, since the optimization task corresponds to identifying its ground-state configurations.

In the context of mapping to a quantum Hamiltonian, the Ising formulation is often more direct. The transformation follows the standard approach of replacing classical spin variables with quantum operators: $s_i \mapsto Z_i$, where Z_i denotes the Pauli-Z operator acting on the i -th qubit. This mapping preserves the eigenvalue structure, with computational basis states $|z\rangle$ corresponding to classical configurations \mathbf{s} (hereinafter, we use the correspondence $0 \leftrightarrow +1$ and $1 \leftrightarrow -1$ between bit and sign variables). The resulting quantum Hamiltonian is constructed as:

$$H_C = \sum_{d=1}^D \sum_{i_1 < \dots < i_d} J_{i_1 \dots i_d} Z_{i_1} \otimes Z_{i_2} \dots \otimes Z_{i_d} \quad (2)$$

This D -local Hamiltonian [42] contains multi-qubit interaction terms that directly encode the higher-order correlations present in the original optimization problem. The ground state of H_C corresponds to the optimal solution, with the ground energy equaling the minimal value of the cost function.

In analyzing HUBO problem complexity, it is essential to consider not only the cardinality of interaction terms but also the topological structure of the underlying hypergraph. Properties such as sparse connectivity, bounded hyperedge size, or specific graph minors can dramatically reduce the effective complexity.

Quantitatively, for $D = 2$ we obtain the QUBO formulation with $O(n^2)$ terms in the worst case, though sparse instances may exhibit only $O(n)$ complexity. For arbitrary order D , the theoretical maximum grows combinatorially as $\sum_{d=1}^D \binom{n}{d}$, creating substantial challenges for classical optimization – particularly when $D > 2$ – despite potential alleviation through structural sparsity [41].

B. XM- and GM-QAOA

QAOA is a hybrid quantum-classical algorithm designed to find approximate solutions to combinatorial optimization problems. The algorithm prepares a parameterized quantum state through the iterative application of two unitary operators derived from problem-specific and mixer Hamiltonians.

The quantum state generated by a p -layer QAOA circuit [shown in Fig. 1(a)] is given by the unitary sequence

$$|\psi(\beta, \gamma)\rangle = U_M(\beta_p)U_C(\gamma_p)\cdots U_M(\beta_1)U_C(\gamma_1)|\psi_0\rangle, \quad U_M(\beta) = e^{-i\beta H_M}, \quad U_C(\gamma) = e^{-i\gamma H_C}. \quad (3)$$

Here, H_C is the cost Hamiltonian encoding the objective function of the optimization problem, such that its ground state corresponds to the optimal solution. The mixer Hamiltonian H_M does not commute with H_C and induces transitions between its eigenstates. The vectors $\beta = (\beta_1, \dots, \beta_p)$ and $\gamma = (\gamma_1, \dots, \gamma_p)$ are the $2p$ variational parameters optimized during the algorithm. The initial state $|\psi_0\rangle$ is chosen to be an energy-extremal eigenstate of H_M .

The mixer Hamiltonian is crucial for exploring the feasible space of the problem. The choice of H_M defines the specific QAOA variant and significantly impacts the algorithm's performance and the reachability of the optimal solution [see Fig. 1(b)].

The most common choice, inspired by quantum annealing, is the transverse-field mixer:

$$H_X = \sum_{i=1}^n X_i \quad (4)$$

where X_j is the Pauli-X operator on qubit j . The resulting unitary,

$$U_X(\beta) = \prod_{j=1}^n e^{-i\beta X_j} \quad (5)$$

implements simultaneous local X -rotations on all qubits. This mixer induces transitions between neighboring states in the computation basis by flipping individual bits, facilitating a local search through the solution space.

An advanced alternative is the Grover-type mixer, which promotes a more global search. It is defined using the projection onto the uniform superposition state $|\text{sym}\rangle = \frac{1}{\sqrt{2^n}} \sum_{\mathbf{s}} |\mathbf{s}\rangle$:

$$H_G = 2|\text{sym}\rangle \langle \text{sym}|. \quad (6)$$

The corresponding unitary evolution operator has the form:

$$U_G(\beta) = e^{-i\beta H_G} = I + (e^{-i2\beta} - 1)|\text{sym}\rangle \langle \text{sym}|, \quad (7)$$

where I stands for the identity matrix. This operator applies a conditional phase shift only to the $|\text{sym}\rangle$ component, effectively performing a selective, global rotation in the Hilbert space. Unlike the local rotations of U_X , U_G can create superpositions and interference patterns that simultaneously involve all possible states.

The fundamental difference between the two mixers lies in their interaction with the cost Hamiltonian. The sequence of $U_X(\beta_k)$ and $U_C(\gamma_k)$ implements a Trotterized approximation of a quantum quench. The local nature of H_X means that the algorithm explores the solution space through a series of local moves, which can be advantageous for problems with a benign, local structure but may lead to slower convergence for problems with complex, long-range correlations. The GM-QAOA ansatz leverages global operations from the outset. The mixer $U_G(\beta_k)$ is equivalent to the diffusion operator in Grover's algorithm. When combined with the phase oracle $U_C(\gamma_k)$, it can amplify the probability amplitude of low-energy states more efficiently for certain problem classes. This can lead to a faster convergence (in terms of the number of layers p) and a higher approximation ratio at fixed p , particularly for problems where the optimal solution is markedly different from the average.

C. Layer-wised optimization

A critical aspect of successfully implementing the QAOA is the efficient optimization of the parameter vectors β and γ . As the number of layers p increases, the optimization landscape becomes more complex, and the task of finding optimal parameters becomes computationally challenging. To address this, a layer-wise optimization strategy is often employed.

The core idea of this strategy is to optimize the parameters incrementally. Instead of optimizing all $2p$ parameters simultaneously for a depth- p circuit, one starts with a single-layer circuit and finds optimal parameters (β_1, γ_1) . These parameters are then held fixed, and a new layer is added. The optimization for depth $i+1$ then proceeds by optimizing only the new parameters $(\beta_{i+1}, \gamma_{i+1})$, initializing them based on the values from the previous layer or a heuristic strategy.

In this work, we use the probability of measuring the ground-state energy, $P(E_{\min})$, as the objective function for optimizing the variational parameters. For a given energy value E , this probability is defined as

$$P(E) = \sum_{\mathbf{s}: E(\mathbf{s})=E} |\langle \mathbf{s} | \psi(\beta, \gamma) \rangle|^2, \quad (8)$$

where $|\mathbf{s}\rangle$ denotes the computational basis state corresponding to the spin configuration \mathbf{s} , and $E_{\min} = \min_{\mathbf{s}} E(\mathbf{s})$ is the minimum value of the cost function. Thus, $P(E_{\min})$ represents the total probability weight that the QAOA output state assigns to all configurations achieving the optimal cost value.

III. COMPARISON ON HUBO PROBLEMS

In this section, we present a systematic comparison between the XM-QAOA and GM-QAOA frameworks applied to two representative combinatorial problems: the Max-Cut problem on random hypergraphs and the Sherrington–Kirkpatrick (SK) spin glass model. Both problems were formulated as HUBO instances of varying locality and system size. For the SK model, all coupling coefficients $J_{i_1 \dots i_d}$ with $d > 1$ were drawn independently from a standard normal distribution (all J_{i_1} are set to zero). For the Max-Cut hypergraph instances, each permissible hyperedge was included independently with probability 1/2, yielding uniformly random binary interaction coefficients $J_{i_1 \dots i_d}$ for $d > 1$. For each problem configuration, 100 random instances were generated and subsequently solved.

Figure 2 illustrates the averaged results for $D = \{2, 4\}$ and $n = \{6, 10, 14\}$. The XM-QAOA curves exhibit rapid initial growth in $P(E_{\min})$ at low circuit depths, but quickly saturate, forming a plateau. This indicates that increasing the number of layers beyond a certain point does not improve solution quality. In contrast, GM-QAOA displays a markedly different behavior: it exhibits a slower, monotonic increase in performance, gradually rising without saturation within the tested range. Notably, the GM-QAOA curve eventually intersects the XM-QAOA plateau at a critical depth (marked with red stars), beyond which it consistently outperforms the transverse-field approach.

Two key trends emerge from the results. First, as the system size n increases, the absolute values of $P(E_{\min})$ decrease for both algorithms, and the critical depth where GM-QAOA surpasses XM-QAOA shifts to larger values. This implies that GM-QAOA requires deeper circuits to outperform XM-QAOA as the problem scale grows.

More importantly, we observe a fundamental difference in how each algorithm responds to increased Hamiltonian locality D . For $D = 2$, XM-QAOA achieves relatively high success probabilities, whereas for $D > 2$, its performance drops significantly and remains consistently low. In stark contrast, GM-QAOA maintains nearly constant performance across different values of D . This resilience to higher-order interactions constitutes the principal advantage of the Grover-style mixer. Specifically, for $D = 4$, the critical depth at which GM-QAOA exceeds the XM-QAOA plateau is approximately three times smaller than for $D = 2$, highlighting its efficiency in tackling high-order optimization problems.

Figure 3 presents an analysis of the same problem instances used in Fig. 2 for two problem classes: Max-Cut (left panels) and the SK model (right panels). The upper panels show the dependence of the averaged critical layer index – defined as the circuit depth beyond which GM-QAOA begins to outperform XM-QAOA – on the system size n for different interaction orders D . The lower panels display the corresponding success probabilities evaluated at these critical depths.

These data reveal several key scaling properties. First, the critical depth exhibits monotonic growth with increasing system size n for both problem types. This indicates that larger systems require deeper quantum circuits to achieve performance superiority of GM-QAOA over XM-QAOA. Notably, this growth is most pronounced for quadratic interactions ($D = 2$), where the critical depth increases rapidly with n . In contrast,

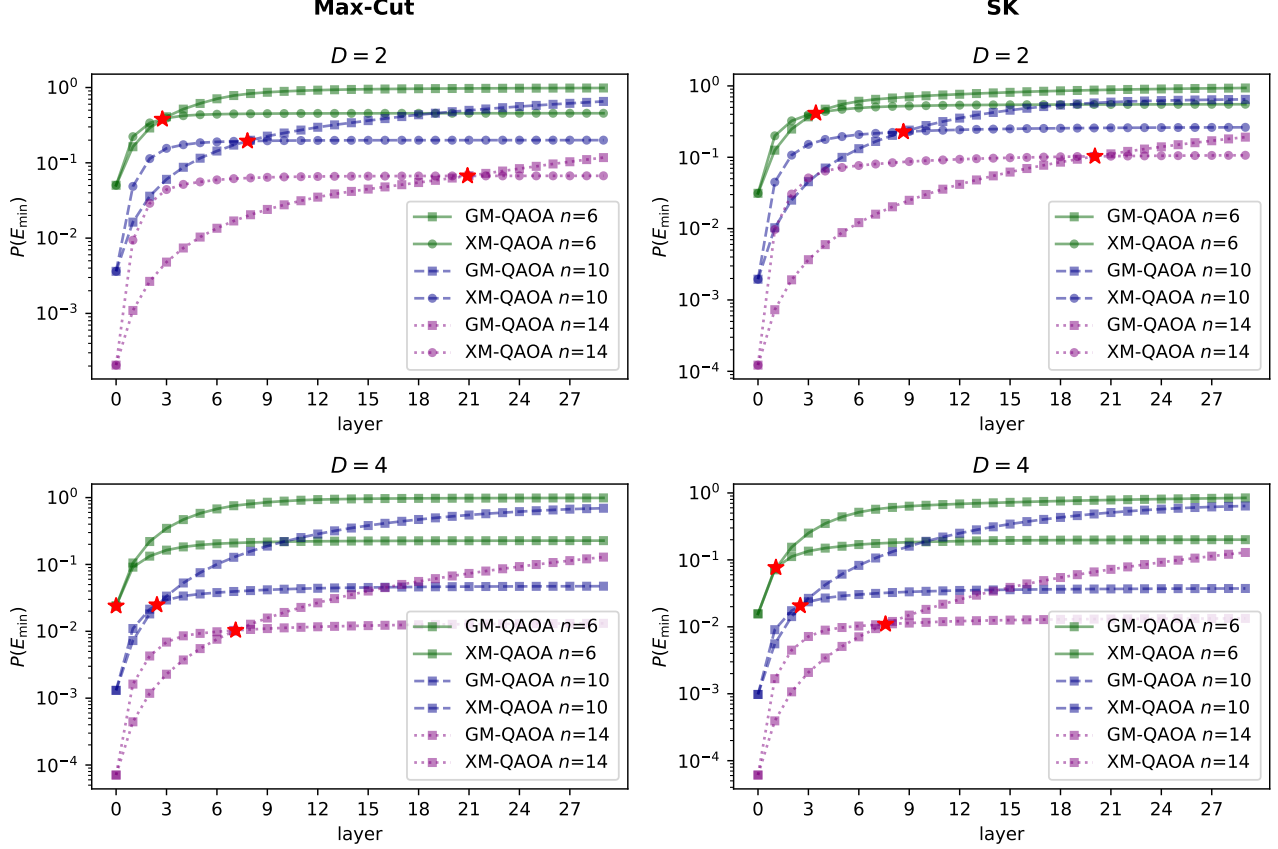


Figure 2: Performance comparison between GM-QAOA and XM-QAOA for the Max-Cut problem on random hypergraphs (left panels) and the (SK) spin glass model (right panels). The plots show the ground-state success probability $P(E_{\min})$ as a function of the circuit depth (layer number) for different system sizes $n \in \{6, 10, 14\}$ and interaction orders $D = 2$ (top row) and $D = 4$ (bottom row). Red stars indicate the minimal circuit depth (critical point) at which GM-QAOA first surpasses the corresponding XM-QAOA performance for each instance family. Each data point represents an average over 100 randomly generated problem instances.

for higher-order interactions ($D = 4$), the required depth remains substantially lower across all system sizes, highlighting the particular efficiency of GM-QAOA for high-degree optimization problems.

The success probability $P(E_{\min})$ at the critical point displays approximately exponential decay with increasing n . This behavior aligns with theoretical expectations for quantum optimization algorithms. Comparative analysis reveals that $P(E_{\min})$ decays more rapidly for hypergraphs with a higher interaction degree, while systems with quadratic interactions maintain higher success probabilities across the studied range of n .

IV. ANALYTICAL APPROXIMATION OF GM-QAOA STATE DYNAMICS

This section introduces a mathematical framework for modeling the layer-wise evolution of GM-QAOA amplitudes, enabling classical pre-optimization of variational parameters. By adopting an energy-resolved representation and assuming a Gaussian distribution of cost-function values, we derive a compact recurrence for the state amplitudes. Combined with an extreme-value-theory estimate of the spectral minimum, the model yields a resource-efficient strategy to determine near-optimal angles without costly quantum evaluations.

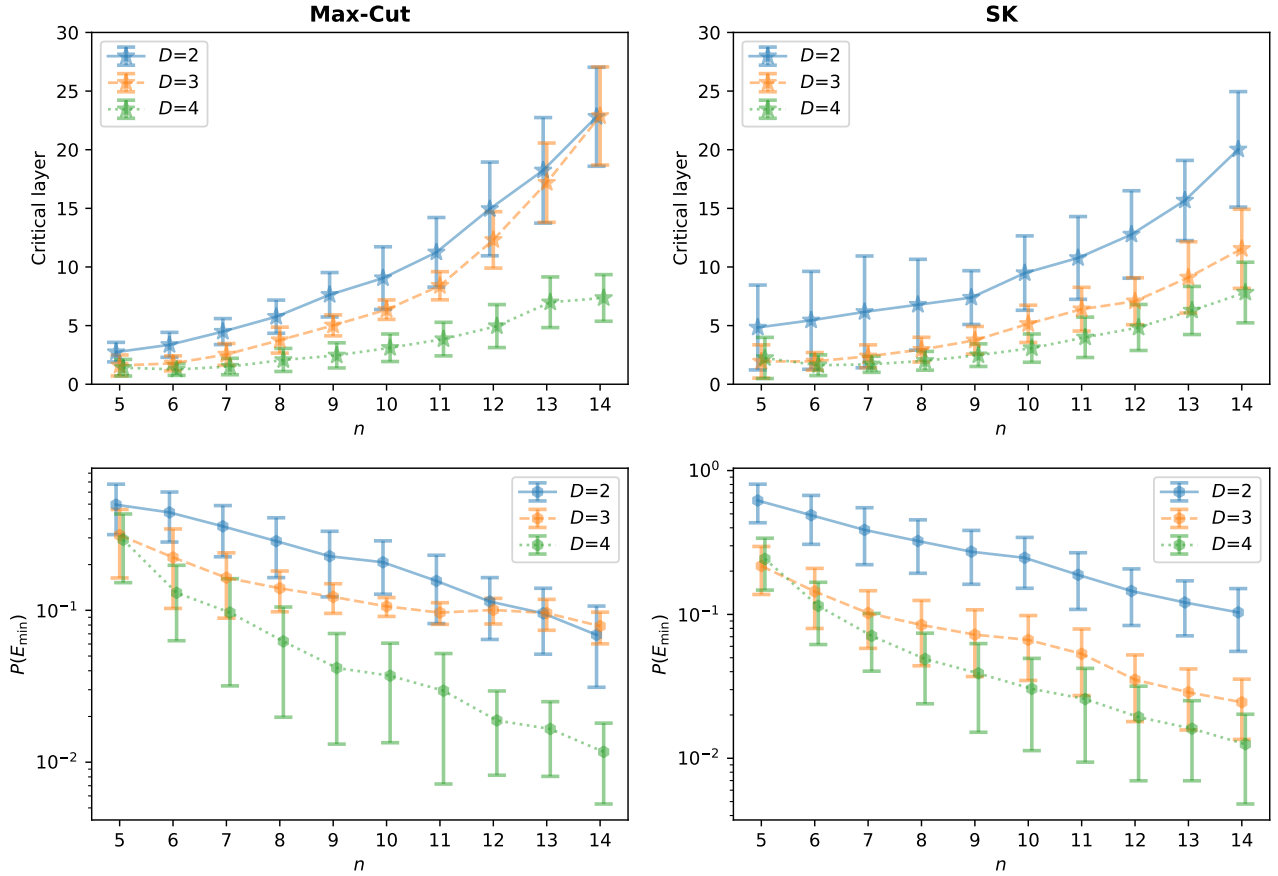


Figure 3: Changing the critical depth, defined as the minimum circuit depth at which GM-QAOA outperforms XM-QAOA, and the corresponding success probability as functions of the problem parameters. Error bars denote the standard deviation over 100 random problem instances.

A. General framework and disorder-averaged dynamics

Consider the quantum state at the k -th layer of GM-QAOA. It can be written as

$$|\beta^{(k)}, \gamma^{(k)}\rangle = \sum_{\mathbf{s}} \Psi_k(\mathbf{s}) |\mathbf{s}\rangle, \quad (9)$$

where $\beta^{(k)} = (\beta_1, \dots, \beta_k)$ and $\gamma^{(k)} = (\gamma_1, \dots, \gamma_k)$ are truncated parameter vectors (the total number of layers is p). The coefficients $\Psi_k(\mathbf{s})$ denote probability amplitudes in the computational basis. Although these amplitudes depend implicitly on $\beta^{(k)}$ and $\gamma^{(k)}$, this dependence is suppressed for notational simplicity.

The initial state corresponds to the uniform superposition, with amplitudes $\Psi_0(\mathbf{s}) = 2^{-n/2}$. Applying a single GM-QAOA layer, consisting of the problem (cost) unitary followed by the Grover-type mixer, leads to the following update rule for the amplitudes:

$$\Psi_k(\mathbf{s}) = (e^{-2i\beta_k} - 1) \Theta_k + e^{-i\gamma_k E(\mathbf{s})} \Psi_{k-1}(\mathbf{s}), \quad (10)$$

where

$$\Theta_k = \frac{1}{2^n} \sum_{\mathbf{s}} e^{-i\gamma_k E(\mathbf{s})} \Psi_{k-1}(\mathbf{s}) \quad (11)$$

is the average amplitude over all computational basis states after applying the problem-specific unitary.

Importantly, the evolution of the amplitudes $\Psi_k(\mathbf{s})$ depends on a basis state \mathbf{s} only through the corresponding value of the cost function $E(\mathbf{s})$. This observation allows us to reparametrize the amplitudes in terms of energy,

$$\Psi_k(\mathbf{s}) \rightarrow \Psi_k(E), \quad (12)$$

which forms the basis for the analytical approximation developed below.

We now treat the cost-function values $E(\mathbf{s})$ for different basis states \mathbf{s} as realizations of a random variable. For a random problem instance, we approximate $E(\mathbf{s})$ as being drawn from a probability distribution $f(E)$. Within this disorder-averaged description, the average amplitude Θ_k can be expressed as an expectation value,

$$\Theta_k \approx \int e^{-i\gamma_k \mathcal{E}} \Psi_{k-1}(\mathcal{E}) f(\mathcal{E}) d\mathcal{E} \equiv \langle e^{-i\gamma_k \mathcal{E}} \Psi_{k-1}(\mathcal{E}) \rangle_{\mathcal{E}}. \quad (13)$$

As a result, we obtain the following recursive relation for the energy-resolved probability amplitudes:

$$\Psi_k(E) = (e^{-2i\beta_k} - 1) \langle e^{-i\gamma_k \mathcal{E}} \Psi_{k-1}(\mathcal{E}) \rangle_{\mathcal{E}} + e^{-i\gamma_k E} \Psi_{k-1}(E). \quad (14)$$

To determine the optimal GM-QAOA parameters γ and β , we maximize the probability of obtaining a low-energy outcome,

$$|\Psi_p(E_{\min}^{\text{est}})|^2 \rightarrow \max, \quad (15)$$

where E_{\min}^{est} denotes an estimate of the location of the minimum energy in the cost-function landscape.

B. Gaussian energy distribution

We now consider the specific case in which the energy distribution $f(E)$ is Gaussian with zero mean and variance σ^2 ,

$$f(E) = \frac{1}{\sqrt{2\pi\sigma^2}} \exp\left(-\frac{E^2}{2\sigma^2}\right). \quad (16)$$

The vanishing mean follows directly from the structure of the cost Hamiltonian H_C , which is assumed to be composed of traceless operators [see Eq. (2)]. Indeed,

$$\langle E(\mathbf{s}) \rangle_{\mathbf{s}} = \frac{1}{2^n} \sum_{\mathbf{s}} E(\mathbf{s}) = \frac{1}{2^n} \text{Tr } H_C = 0. \quad (17)$$

The variance σ^2 is determined by the second moment of the energy distribution and can be expressed as

$$\sigma^2 = \langle E^2(\mathbf{s}) \rangle_{\mathbf{s}} = \frac{1}{2^n} \text{Tr}(H_C^2) = \sum_{d=1}^D \sum_{i_1 < \dots < i_d} J_{i_1 \dots i_d}^2, \quad (18)$$

where D denotes the maximum interaction order of the cost Hamiltonian.

Substituting the Gaussian distribution into the recursive relation Eq. (14), we find that the probability amplitude at layer k admits the following decomposition:

$$\Psi_k(E) = A_k + B_k(E), \quad (19)$$

where A_k is an energy-independent contribution, while $B_k(E)$ captures the explicit energy dependence.

For $k \geq 1$, these terms take the form

$$A_k = (e^{-2i\beta_k} - 1) \sum_{i=1}^k \exp\left[-\frac{\sigma^2}{2} (\gamma_k^2 + \gamma_{k-1}^2 + \dots + \gamma_{k-i+1}^2)\right] A_{k-i}, \quad (20)$$

and

$$B_k(E) = \sum_{j=1}^k A_{k-i} \exp[-i(\gamma_k + \gamma_{k-1} + \dots + \gamma_{k-j+1}) E], \quad (21)$$

with the initial conditions $A_0 = 2^{-n/2}$ and $B_0(E) = 0$.

C. Minimum energy approximation

The recursive formulation of multi-layer GM-QAOA dynamics requires an estimate of the location of the minimum energy E_{\min} , which serves as a target value in the optimization of the final-state probability distribution. Since the exact ground-state energy is generally unknown, we employ tools from extreme value theory (EVT) to obtain a statistically motivated estimate based on an assumed distribution of energy levels.

EVT provides a rigorous framework for characterizing the statistics of extrema of large samples of random variables. According to the Fisher–Tippett–Gnedenko theorem [43, 44], properly normalized extrema of independent and identically distributed random variables converge to one of three universal distributions, collectively described by the generalized extreme value (GEV) distribution [45–49],

$$G(x) = \exp \left\{ - \left[1 + \xi \left(\frac{x - \tilde{\mu}}{\tilde{\sigma}} \right) \right]^{-1/\xi} \right\}, \quad 1 + \xi \left(\frac{x - \tilde{\mu}}{\tilde{\sigma}} \right) > 0, \quad (22)$$

where $\tilde{\mu}$ is the location parameter, $\tilde{\sigma} > 0$ is the scale parameter, and ξ is the shape parameter determining the distribution class. The cases $\xi = 0$, $\xi > 0$, and $\xi < 0$ correspond to the Gumbel, Fréchet, and Weibull distributions, respectively.

Although EVT is conventionally formulated for maxima, the statistics of minima can be obtained by applying the theory to the random variable $-E$. For energy levels modeled as independent Gaussian random variables, $E \sim \mathcal{N}(\mu, \sigma^2)$ (in our case $\mu = 0$), the distribution belongs to the Gumbel universality class, i.e., $\xi = 0$.

The probability density function of the Gumbel distribution for the minimum energy is then given by

$$f_G(x) = \frac{1}{\beta_G} \exp \left(\frac{x - \mu_G}{\beta_G} - e^{\frac{x - \mu_G}{\beta_G}} \right), \quad (23)$$

where the location and scale parameters are expressed in terms of order statistics of N independent Gaussian samples as

$$\mu_G = \mu + \sigma \Phi^{-1} \left(\frac{1}{N} \right), \quad \beta_G = \sigma \left[\Phi^{-1} \left(\frac{1}{N} \right) - \Phi^{-1} \left(\frac{1}{eN} \right) \right]. \quad (24)$$

Here $N = 2^n$ denotes the total number of computational basis states, and Φ^{-1} is the quantile function of the standard normal distribution.

We use the mode of the Gumbel distribution as an estimate of the minimum energy, which directly yields

$$E_{\min}^{\text{est}} = \mu_G = \sigma \Phi^{-1} \left(\frac{1}{2^n} \right). \quad (25)$$

This estimate provides a simple and analytically tractable target energy for GM-QAOA parameter optimization, while correctly capturing the exponential growth of the effective search space with system size under the Gaussian energy approximation.

A closely related estimate was introduced in Ref. [21] for Ising problems with normally distributed couplings. In that work, the authors also proposed an explicit large- n approximation to the Gaussian quantile, which leads to the expression

$$E_{\min}^{\text{est}} \approx -\sigma \sqrt{2 \ln 2} \sqrt{n} \left(1 + \frac{1}{4 \ln 2} \frac{\ln n}{n} \right)^{-1}, \quad (26)$$

reproducing the leading random-energy-model scaling $E_{\min} \sim -\sigma \sqrt{2n \ln 2}$. This closed-form approximation is particularly convenient when numerical evaluation of Φ^{-1} is impractical.

V. PERFORMANCE ANALYSIS

In this section, we present a resource-efficient strategy for selecting GM-QAOA parameters that avoids extensive quantum hardware runtime. The approach builds upon the analytical framework developed in the previous sections, combined with the extreme-value-theory-based estimate of the minimum energy E_{\min}^{est} , and enables classical pre-optimization of the variational parameters $\{\beta_k, \gamma_k\}$.

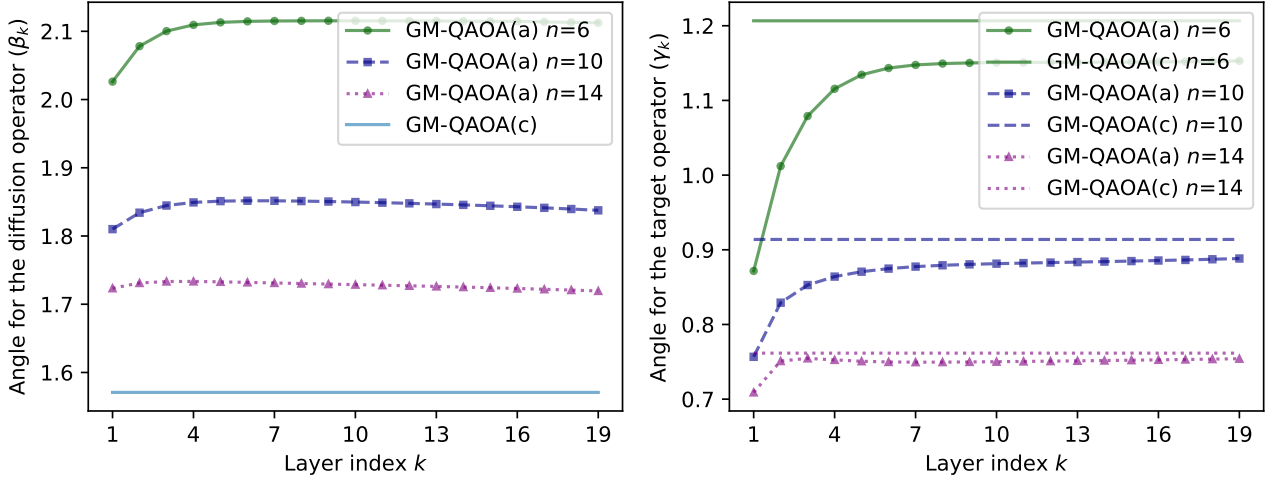


Figure 4: Comparison of analytically optimized parameters β_k (left panel) and γ_k (right panel) as functions of the layer index k for GM-QAOA(a), contrasted with the constant-angle variant GM-QAOA(c) introduced in Ref. [21]. The data are averaged over 100 random SK instances with HUBO order $D = 2$ (corresponding to the Ising case) for each system size n .

The central idea is to maximize the analytically derived probability $P(E_{\min}^{\text{est}})$ of obtaining the minimum-energy configuration as a function of the circuit parameters. This is achieved via a layer-by-layer numerical optimization of $P(E_{\min}^{\text{est}})$, using the expressions for the two contributions to the probability amplitudes given in Eqs. (20) and (21). The resulting optimized angles can then be directly used in GM-QAOA circuits executed on quantum hardware, thereby reducing or completely eliminating the need for iterative hybrid optimization. In what follows, we refer to this analytically optimized variant as GM-QAOA(a).

We also compare our approach with the simplified GM-QAOA scheme introduced in Ref. [21], where the circuit parameters are fixed rather than optimized. In that work, the authors considered the choice

$$\beta_k = \frac{\pi}{2}, \quad \gamma_k = -\frac{\pi}{E_{\min}^{\text{est}}}, \quad (27)$$

for all layers k . This parameterization closely parallels Grover's search algorithm: the choice $\beta_k = \pi/2$ plays the role of the Grover diffusion operator, while $\gamma_k = -\pi/E_{\min}^{\text{est}}$ induces a phase shift of approximately -1 on the target (minimum-energy) state. We refer to this constant-angle variant as GM-QAOA(c).

To study analytically optimized angle selection, we consider ensembles of SK problem instances with interaction orders $D = 2, 3, 4$ and system sizes $n = 5, \dots, 14$. For each pair (D, n) , we generate 100 random instances. We focus on SK problems because their coupling coefficients are drawn from a normal distribution, which naturally supports the Gaussian approximation of the energy spectrum underlying our extreme-value-theory-based analysis.

In Fig. 4, we compare the optimized angle values $\{\gamma_k, \beta_k\}$ obtained from the analytical optimization procedure with the constant-angle choice defined in Eq. (27) for $D = 2$. The comparison reveals several notable features. First, the optimal mixing angle β_k in the analytically optimized scheme is not constant but exhibits a clear dependence on the system size n . Its asymptotic value at large n deviates significantly from $\pi/2$, approaching a substantially larger value. Second, while the asymptotic behavior of the phase angles γ_k shows reasonable agreement between the two approaches, the key difference lies in their layer-wise structure. In contrast to the constant-parameter baseline, the analytically optimized angles are strongly layer dependent: both β_k and γ_k undergo pronounced adjustments in the initial layers of the circuit before converging to steady-state values at larger depths. This nontrivial parameter scheduling in the early stages of the algorithm plays a crucial role in enhancing performance.

Next, we compare the performance of XM- and GM-QAOA with layer-wise optimization, introduced earlier, against two analytical approaches – one with parameter optimization and one without. Illustrative results are shown in Fig. 5.

Several key conclusions can be drawn from these results. First, the analytically optimized approach [GM-QAOA(a)] consistently outperforms its non-optimized counterpart [GM-QAOA(c)], highlighting the importance of classical pre-optimization of the mixing angles β_k . Second, as the locality of the cost Hamiltonian increases

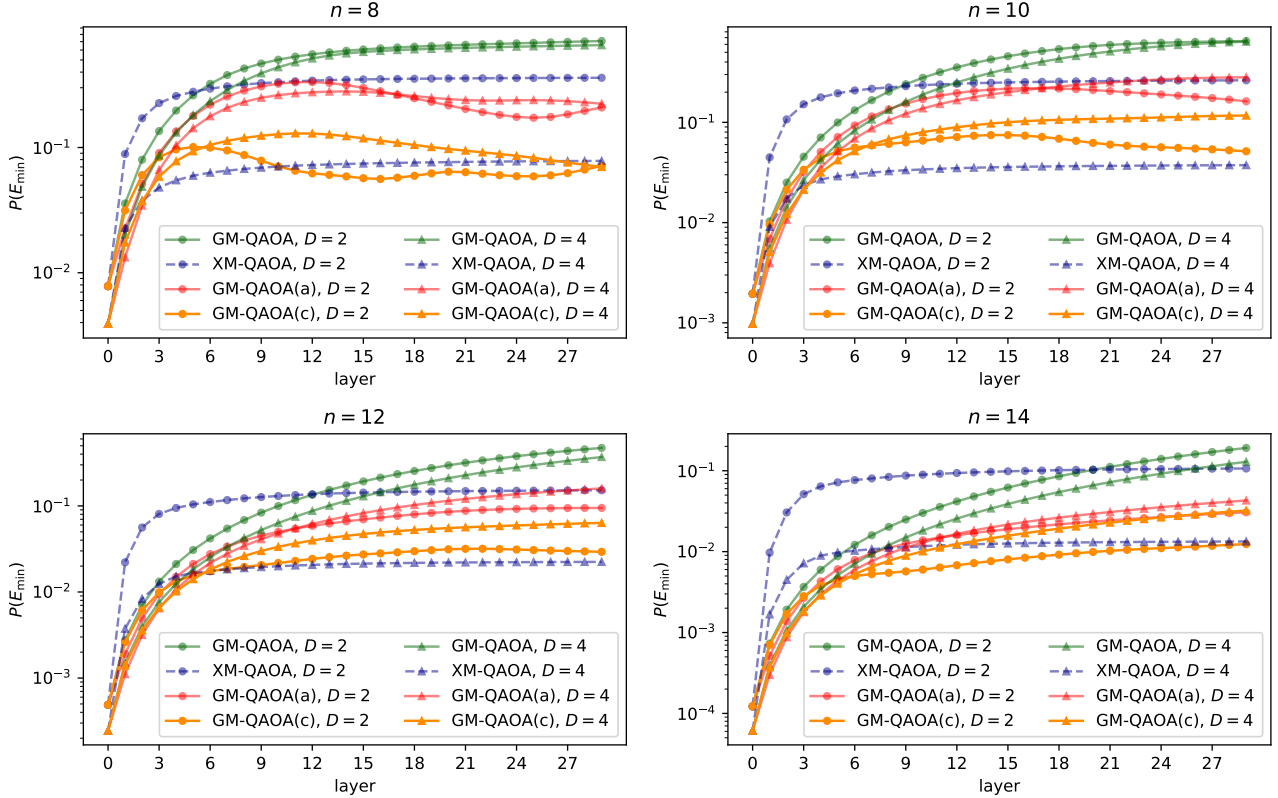


Figure 5: Behavior of the success probability $P(E_{\min})$ as a function of the number of layers for four methods: layer-wise optimized GM-QAOA, XM-QAOA, and two analytical approaches—one with parameter optimization [GM-QAOA(a)] and one without [GM-QAOA(c)]—for various problem sizes n and HUBO orders D .

the performance of GM-QAOA(a) improves significantly, approaching that of the fully layer-wise optimized GM-QAOA while requiring substantially fewer quantum resources. Notably, for $D = 4$ we observe that beyond a certain circuit depth the analytically optimized variant GM-QAOA(a) begins to outperform XM-QAOA. We also note that for fully layer-wise optimized GM-QAOA, increasing the locality from $D = 2$ to $D = 4$ leads to a degradation of the success probability $P(E_{\min})$. In contrast, for the analytically motivated approaches this trend is reversed, with higher-order interactions yielding improved performance. This behavior suggests that analytical angle selection becomes increasingly advantageous as the locality of the cost Hamiltonian grows.

To conclude our analysis, we investigate the behavior of the crossover point, defined as the critical circuit depth (layer index) beyond which GM-QAOA begins to outperform XM-QAOA in terms of the success probability $P(E_{\min})$, averaged over problem instances. Figure 6 shows the critical circuit depths at which the analytically optimized GM-QAOA(a) surpasses the performance plateau of XM-QAOA. For the case of pairwise interactions ($D = 2$), no such crossover is observed within the considered range of system sizes, and XM-QAOA consistently outperforms GM-QAOA(a) for all n . The observed behavior exhibits the same qualitative characteristics as the fully optimized GM-QAOA implementation. In particular, the critical depth increases monotonically with the problem size n while displaying an inverse dependence on the interaction order D of the cost Hamiltonian.

VI. CONCLUSIONS

In this work, we have systematically investigated the application of GM-QAOA to HUBO problems. Our results demonstrate that the GM-QAOA framework, owing to its global mixing mechanism, offers a distinct advantage over XM-QAOA for optimization problems involving high-order interactions. In particular, we have shown that while XM-QAOA exhibits an early performance plateau at shallow circuit depths, GM-QAOA displays a monotonic improvement with increasing depth and ultimately surpasses XM-QAOA beyond a critical layer. This advantage becomes increasingly pronounced as the locality D of the cost Hamiltonian grows, highlighting the robustness of GM-QAOA against the complexity induced by multi-spin correlations.

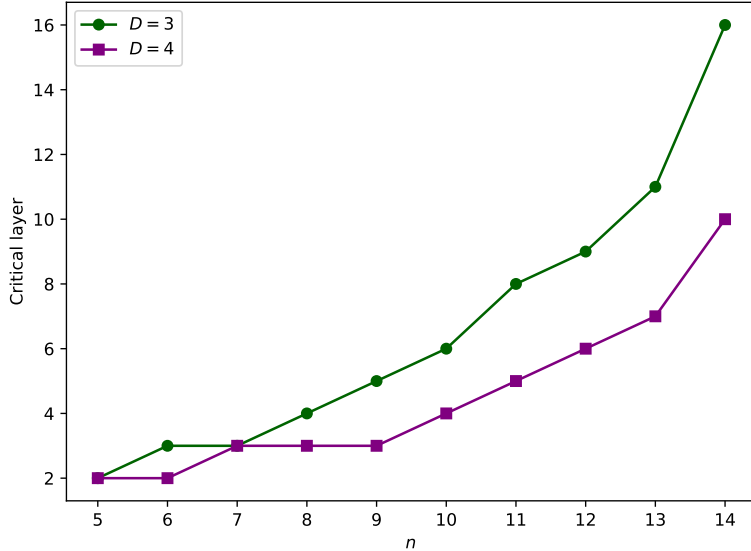


Figure 6: Minimum circuit depth at which GM-QAOA(a) outperforms XM-QAOA in terms of the success probability $P(E_{\min})$ as a function of the number of qubits n for $D = 3, 4$.

A key contribution of this study is the development of an analytical model for GM-QAOA dynamics with variable mixing angles. Building on this model, we introduced a resource-efficient parameter selection strategy based on classical pre-optimization. We demonstrated that the resulting analytically optimized variant, GM-QAOA(a), can achieve performance close to that of the fully optimized GM-QAOA, while substantially reducing the required quantum resources. This establishes GM-QAOA(a) as a practical and scalable approach for high-order optimization problems.

Several promising directions for future research naturally follow from our results. First, extending the present analytical framework to alternative mixer Hamiltonians and broader classes of optimization problems, including constrained settings, could further enhance the versatility of QAOA-based approaches. Second, an experimental realization of GM-QAOA for HUBO problems on qudit-based quantum processors represents an important next step toward practical validation, particularly in view of the more compact and native encodings enabled by multi-level systems. Finally, a promising avenue for future study is the development of fixed-point strategies that simultaneously scale the system size and circuit depth, while employing low-dimensional parametrizations of the variational parameters [50]. Taken together, these directions suggest that the proposed framework contributes to advancing quantum optimization toward practical relevance for complex, large-scale problems.

ACKNOWLEDGMENTS

This research was supported by the Priority 2030 program at the National University of Science and Technology “MISIS” under the project K1-2022-027.

[1] K. Bharti, A. Cervera-Lierta, T. H. Kyaw, T. Haug, S. Alperin-Lea, A. Anand, M. Degroote, H. Heimonen, J. S. Kottmann, T. Menke, *et al.*, *Reviews of Modern Physics* **94**, 015004 (2022).

[2] M. Cerezo, A. Arrasmith, R. Babbush, S. C. Benjamin, S. Endo, K. Fujii, J. R. McClean, K. Mitarai, X. Yuan, L. Cincio, *et al.*, *Nature Reviews Physics* **3**, 625 (2021).

[3] J. Biamonte, P. Wittek, N. Pancotti, P. Rebentrost, N. Wiebe, and S. Lloyd, *Nature* **549**, 195 (2017).

[4] S. McArdle, S. Endo, A. Aspuru-Guzik, S. C. Benjamin, and X. Yuan, *Reviews of Modern Physics* **92**, 015003 (2020).

[5] X. Yuan, S. Endo, Q. Zhao, Y. Li, and S. C. Benjamin, *Quantum* **3**, 191 (2019).

[6] X. Xu, J. Sun, S. Endo, Y. Li, S. C. Benjamin, and X. Yuan, *Science Bulletin* **66**, 2181 (2021).

[7] A. K. Fedorov, N. Gisin, S. M. Belousov, and A. I. Lvovsky, *arXiv preprint arXiv:2203.17181* (2022).

[8] E. Farhi, J. Goldstone, and S. Gutmann, *arXiv preprint arXiv:1411.4028* (2014).

- [9] E. Farhi and A. W. Harrow, arXiv preprint arXiv:1602.07674 (2016).
- [10] G. Pagano, A. Bapat, P. Becker, K. S. Collins, A. De, P. W. Hess, H. B. Kaplan, A. Kyprianidis, W. L. Tan, C. Baldwin, *et al.*, Proceedings of the National Academy of Sciences **117**, 25396 (2020).
- [11] M. P. Harrigan, K. J. Sung, M. Neeley, K. J. Satzinger, F. Arute, K. Arya, J. Atalaya, J. C. Bardin, R. Barends, S. Boixo, *et al.*, Nature Physics **17**, 332 (2021).
- [12] L. Zhou, S.-T. Wang, S. Choi, H. Pichler, and M. D. Lukin, Physical Review X **10**, 021067 (2020).
- [13] L. K. Grover, in *Proceedings of the twenty-eighth annual ACM symposium on Theory of computing* (1996) pp. 212–219.
- [14] A. Bärtschi and S. Eidenbenz, in *2020 IEEE International Conference on Quantum Computing and Engineering (QCE)* (IEEE, 2020) pp. 72–82.
- [15] G. A. Bridi and F. d. L. Marquezino, Physical Review A **110**, 052409 (2024).
- [16] N. Xie, J. Xu, T. Chen, X. Lee, Y. Saito, N. Asai, and D. Cai, Physical Review A **111**, 012401 (2025).
- [17] J. Golden, A. Bärtschi, D. O’Malley, and S. Eidenbenz, in *2021 IEEE International Conference on Quantum Computing and Engineering (QCE)* (IEEE, 2021) pp. 137–147.
- [18] N. Benchasattabuse, A. Bärtschi, L. P. García-Pintos, J. Golden, N. Lemons, and S. Eidenbenz, arXiv preprint arXiv:2308.15442 (2023).
- [19] E. Pelofske, Physical Review E **111**, 054103 (2025).
- [20] T. Y. Ng, J. M. Koh, and D. E. Koh, arXiv preprint arXiv:2411.09745 (2024).
- [21] A. Zhukov, A. Lebedev, and W. Pogosov, Computer Physics Communications , 109627 (2025).
- [22] B. Tsvelikhovskiy, M. Nuyten, and B. N. Bakalov, arXiv preprint arXiv:2509.10424 (2025).
- [23] E. O. Kiktenko, A. S. Nikolaeva, P. Xu, G. V. Shlyapnikov, and A. K. Fedorov, Physical Review A **101**, 022304 (2020).
- [24] A. S. Nikolaeva, E. O. Kiktenko, and A. K. Fedorov, Physical review A **105**, 032621 (2022).
- [25] E. O. Kiktenko, A. S. Nikolaeva, and A. K. Fedorov, Reviews of Modern Physics **97**, 021003 (2025).
- [26] A. S. Nikolaeva, E. O. Kiktenko, and A. K. Fedorov, EPJ Quantum Technology **11**, 1 (2024).
- [27] A. S. Nikolaeva, I. V. Zalivako, A. S. Borisenko, N. V. Semenin, K. P. Galstyan, A. E. Korolkov, E. O. Kiktenko, K. Y. Khabarova, I. A. Semerikov, A. K. Fedorov, *et al.*, Physical Review Letters **135**, 060601 (2025).
- [28] J. Chu, X. He, Y. Zhou, J. Yuan, L. Zhang, Q. Guo, Y. Hai, Z. Han, C.-K. Hu, W. Huang, *et al.*, Nature physics **19**, 126 (2023).
- [29] D. A. Chermoshentsev, A. O. Malyshev, M. Esencan, E. S. Tiunov, D. Mendoza, A. Aspuru-Guzik, A. K. Fedorov, and A. I. Lvovsky, arXiv preprint arXiv:2106.13167 (2021).
- [30] I. G. Rosenberg, Cahiers du Centre d’Études de Recherche Opérationnelle **17**, 71 (1975).
- [31] E. Boros and A. Gruber, arXiv preprint arXiv:1404.6538 (2014).
- [32] A. Semenov, S. Usmanov, and A. Fedorov, Problems of Information Transmission **61**, 110 (2025).
- [33] N. Dattani, arXiv preprint arXiv:1901.04405 (2019).
- [34] T. J. Sejnowski *et al.*, in *AIP Conference Proceedings*, Vol. 151 (American Institute of Physics, 1986) pp. 398–403.
- [35] T. G. Kolda and B. W. Bader, SIAM review **51**, 455 (2009).
- [36] C.-C. Chang and C.-J. Lin, ACM transactions on intelligent systems and technology (TIST) **2**, 1 (2011).
- [37] W.-H. Wei, G. Hemani, and C. S. Haley, Nature Reviews Genetics **15**, 722 (2014).
- [38] M. L. Klein and W. Shinoda, science **321**, 798 (2008).
- [39] C. C. Ribeiro, D. Aloise, T. F. Noronha, C. Rocha, and S. Urrutia, European Journal of Operational Research **191**, 981 (2008).
- [40] C. Bierwirth and D. C. Mattfeld, Evolutionary computation **7**, 1 (1999).
- [41] R. Shaydulin, C. Li, S. Chakrabarti, M. DeCross, D. Herman, N. Kumar, J. Larson, D. Lykov, P. Minssen, Y. Sun, *et al.*, Science Advances **10**, eadm6761 (2024).
- [42] J. Kempe, A. Kitaev, and O. Regev, Siam journal on computing **35**, 1070 (2006).
- [43] R. A. Fisher and L. H. C. Tippett, in *Mathematical proceedings of the Cambridge philosophical society*, Vol. 24 (Cambridge University Press, 1928) pp. 180–190.
- [44] B. Gnedenko, Annals of mathematics **44**, 423 (1943).
- [45] A. F. Jenkinson, Quarterly Journal of the Royal meteorological society **81**, 158 (1955).
- [46] J. Pickands III, the Annals of Statistics , 119 (1975).
- [47] S. Coles, J. Bawa, L. Trenner, and P. Dorazio, *An introduction to statistical modeling of extreme values*, Vol. 208 (Springer, 2001).
- [48] J. Beirlant, Y. Goegebeur, J. Segers, and J. L. Teugels, *Statistics of extremes: theory and applications* (John Wiley & Sons, 2006).
- [49] L. Haan and A. Ferreira, *Extreme value theory: an introduction*, Vol. 3 (Springer, 2006).
- [50] A. Y. Chernyavskiy, D. Kulikov, B. Bantysh, Y. I. Bogdanov, A. Fedorov, and E. Kiktenko, arXiv preprint arXiv:2509.19035 (2025).